

Effect of agglomerated zirconia-toughened mullite on the mechanical properties of giant cane fiber mat epoxy laminated composites

Pruthwiraj Sahu^{*1}, Sambit Kumar Parida^{2a} and Sisir Mantry^{3b}

¹School of Mechanical Engineering, KIIT, Bhubaneswar: 751024, Odisha, India

²Department of Manufacturing Engineering, NIFFT Ranchi: 834003, Jharkhand, India

³Institute of Minerals and Materials Technology, Bhubaneswar: 751013, Odisha, India

(Received December 13, 2018, Revised February 14, 2019, Accepted February 20, 2019)

Abstract. This paper depicts the development and characterizations of laminated composites made with cellulosic giant cane (*Arundinaria gigantea*) fiber mats and epoxy resin. Zirconia-toughened mullite (ZTM) is used as a filler material in the laminated composite which was prepared from sillimanite through plasma processing technique. The mechanical characterizations of this composite have been carried out as per ASTM standards to evaluate its usability as a structural material. The effects of varying weight percentages of the filler and two different fiber orientations namely, angle-ply [$+45^\circ/-45^\circ/+45^\circ$] and balanced cross-ply [$0^\circ/90^\circ/0^\circ$] on the physical and mechanical properties such as density, microhardness, impact strength, tensile strength and interlaminar shear strength of the layered composite specimens have been investigated. The study indicates that the inclusion of zirconia-toughened mullite in the composite laminate as filler improves its mechanical properties. Moreover, the use of giant cane fiber mat in the laminate is more eco-friendly than the synthetic fibers. This research also helps in generating additional data to enrich the repository of natural fiber reinforced laminated composites.

Keywords: giant cane (*arundinaria gigantea*) fiber mat; zirconia-toughened mullite; laminated composites; mechanical characterization; fiber orientations

1. Introduction

Natural fiber reinforced polymer composites (NFRPC) made from giant cane fiber mats are considered as a potential substitute of the synthetic fibers like glass, carbon, aramid, etc. These fibers are bio-degradable and possess very good tensile and flexure strength, because of the presence of high volume of longitudinally oriented cellulosic fiber (α -cellulose) in them. Gurunathan *et al.* (2015) presented a detailed overview of the development of bio-composites from several natural fibers. The treatment of natural fibers by suitable chemical reagents like NaOH, trimethoxysilane removes the oily and sticky materials like pectin from the natural fibers. Thus, the NaOH treatment of fibers enhances the physico-mechanical, tribological and thermal properties because of the improvement of the adhesion characteristics of the fiber matrix interface (Satapathy *et al.* 2010, Sepe *et al.* 2018, Yan *et al.* 2016). The cellulosic fibers such as jute, coir, bamboo have good mechanical strength. The strength of these fibers is comparable to the strength of many other synthetic fibers because of the rich content of aligned cellulosic fibers in

them. Several works focusing on the development, mechanical characterization and studying the water absorption capacity of the composite laminates made from both 5% NaOH alkali treated and untreated bamboo fibers have been reported (Manalo *et al.* 2015, Mir *et al.* 2013, Jena *et al.* 2013, Kushwaha *et al.* 2008, Bisen *et al.* 2018) studied the effect of fiber volume fractions on the elastic properties of natural fiber (Luffa fiber) reinforced epoxy composite by varying the weight percentage of treated Luffa fiber. Biswas *et al.* (2011) investigated the influence of both fiber content and fiber orientations on mechanical and erosion behavior of glass fiber-reinforced epoxy composites. Kim *et al.* (2018) observed that the flexural strength and toughness increased proportionally with the steel-fiber volume fraction in fiber-reinforced cementitious composites based on slurry-infiltrated fiber concrete (SIFCON-based HPFRCC). Perrier *et al.* (2017) have investigated the effect of hygroscopic loading on damage initiation mechanics in woven hemp/epoxy composites during tensile loading. Cunha *et al.* (2008) studied numerically the mechanical behavior of pultruded glass fiber reinforced plastic (GFRP) for beam and shell finite element. Further, the fabrication and testing of composite made from alkali and silane treated hemp fibers (both short and long treated) in poly(lactic acid) matrix has shown the improvement of the tensile and impact properties due to improved adhesion with matrix and improved crystallinity of the poly(lactic acid) (Sawpan *et al.* 2011).

The pioneering work regarding the suitability of using Arundo Donax L. (giant cane) fibers as reinforcement in FRP composite was investigated through tensile test of

*Corresponding author, Research Scholar
E-mail: psahumech.fme@kiit.ac.in

^aAssistant Professor
E-mail: sambitparida@gmail.com

^bScientist
E-mail: mantrysisir@gmail.com

single sand fiber (Fiore *et al.* 2014). The researchers reported that the giant cane fiber is quite suitable material and their properties are comparable to the bamboo fibers. Scalici *et al.* (2016) reported the influence of plasma treatment on the properties of natural fiber composite made from the leaves of the giant reed *Arundo Donax L.* and evaluated the mechanical performance of the composite under static and dynamic conditions. The plasma treatment of these fibers improves fiber/matrix adhesion as revealed from the SEM micrographs. The effects of chemical modification by varying concentrations of NaOH solution and different silane coupling agents of fiber surface in sisal–oil palm reinforced natural rubber green composites have also been studied (John *et al.* 2008). Further, the use of giant cane fiber as a filler material in hot mix of asphalt used in construction of road and pavement has been experimented by Karahancer *et al.* (2016), and inferred that the addition these fibers reduces the susceptibility of water absorption of the pavement.

Fiore *et al.* (2014a) prepared a new class of composite from the grinded giant cane fiber as reinforcement in the epoxy resins and studied the influence of the fiber content and size of chopped fibers on the mechanical properties in static and dynamic conditions. Further, it was also reported that the addition of *Arundo Donax* filler (ADF) significantly influences the thermo-mechanical properties of bio-composites made from polylactic acid (PLA) as matrix (Fiore *et al.* 2014b). Moreover, the flexural strength of the slabs made with plaster and common reed (giant cane fiber) for various designs have been tested and compared with that obtained from the traditional design. Gabarron *et al.* (2014) observed that the flexural strength of the slabs increased up to 116.2% (5.34 N/mm²) with respect to the traditional design (2.47 N/mm²). A detailed account of the usability of the natural fibers and natural fiber composites in different commercial and structural applications has been presented by Sanjay *et al.* (2016). Gonçalves *et al.* (2015) described the in-plane cyclic behavior of timber framed masonry walls with controlled displacements. Further, Cruz *et al.* (2015) ascertained that the layered composite made from giant bamboo fibers not only exhibits better ballistic performance in practical application such as portable armor for personal protection but is also lighter and has economic advantages over the composites made from aramid fabric.

Several works analyzing the dynamic stability, vibration analysis, bending and buckling of laminated sandwich structure reinforced with single walled carbon nanotubes (SWCNTs) and carbon fiber have been reported (Kolahchi *et al.* 2016a, b, Arani *et al.* 2016, Hajmohammada *et al.* 2018a, b, Shokravi 2017, Bilouei *et al.* 2016). Moreover, the dynamic buckling analysis and vibration analysis of piezoelectric sandwich nanocomposite plates has also been carried out by various researchers (Kolahchi *et al.* 2016c, Kolahchi *et al.* 2017a, b, c, Hajmohammad *et al.* 2018c, Hajmohammad *et al.* 2017a). In addition, numerical study on the dynamic pull-in and pull-out behaviour of embedded nano-sandwich plates alongside the seismic response of underwater fluid-conveying concrete pipes has also been carried out (Hajmohammad *et al.* 2018d, e, Shokravi 2017, Kolahchi 2017d). Further, the influence of agglomerated

SiO₂ nanoparticles on the dynamic behaviour of non-homogenous concrete blocks, pipes and columns subjected to different types of load has been investigated (Amnieh *et al.* 2018, Zarei *et al.* 2017, Zamanian *et al.* 2017).

It is well known that the customized mechanical properties of the materials can be obtained depending on the application by suitable combination of the parameters such as fiber volume fraction and orientation angle, number of layers and the weight percentages of the filler. From this brief review of literature, it is evident that the studies (experimental/analytical/numerical) investigating the influence of ZTM filler on the mechanical properties of natural cane fiber composite are scarce. Moreover, ZTM is an industrial waste and degrades air quality. The composite laminates made from giant cane fibers and ZTM filler can find potential applications in automobile dashboard, roof, rear wall, side panel lining, shipping pallets, furniture, and household products. This could open an outlet for utilizing the industrial waste (mullite) in the aforementioned areas thereby mitigating its adverse effect on the environment provided its influence on the mechanical properties is ascertained.

Therefore, the objective of this work is to investigate the improvement of mechanical strength by including the ZTM as filler with natural giant cane fiber composite. The following few sets of work has been completed and presented in detail. Firstly, the laminated composites have been fabricated by using cellulosic giant cane (*Arundinaria gigantea*) fiber mats and epoxy resin via hand lay-up technique. The ZTM obtained from sillimanite through plasma processing technique, is used as the filler material. Subsequently, the physical and mechanical properties i.e., density, tensile strength, interlaminar shear strength, impact strength and microhardness of the composite laminates have been evaluated experimentally by following the ASTM standards. Finally, the influence of varying weight percentages of the filler (ZTM), ply sequence and chemical treatment (NaOH bath) of giant cane fiber mats on the said mechanical properties of natural fiber-reinforced layered composite is studied via numerous experimentations and discussed in detail in the following sections.

2. Materials and methods

2.1 Giant cane fiber mat

Giant cane (river cane, wild cane, spanish cane, giant reed or *Arundo Donax L.*) is cultivated in the state of Assam (a north eastern state of India). The giant cane belongs to the family Poaceae, genus *Arundinaria* and species *Arundinaria gigantea*. The fiber mats are woven from the thin strips taken out from the woody stem of the seasoned giant cane plants. The seasoned and dried fibers have better dimensional stability as they don't shrink much after fabrication (Fiore *et al.* 2014). The composition and properties of *Arundo* fibers and some natural fibers (Perrier *et al.* 2017) are presented in Table 1. It is to be marked that the density of giant cane fiber is 1168 kg/m³ and the tensile strength is 248 MPa, which is comparable to that of the bamboo fiber (Fiore *et al.* 2014). Consequently, the

Table 1 Composition and properties of Arundo Donax L. fibers and some natural fibers (Perrier *et al.* 2017)

Fiber	Cellulose (%wt.)	Hemi cellulose (%wt.)	Lignin (%wt.)	Density (kg/m ³)	Tensile strength (MPa)	Young's modulus (GPa)	Elongation at break (%)
Sisal	78	10	8	1500	511-635	9.4-22	2.25
Coir	43	0.3	45	1200	175	4-6	30
Jute	72	13	13	1300	393-773	26.5	1.5-1.8
Flax	81	16.7-20.6	3	1500	345-1035	27.6	2.7-3.2
Bamboo	26-43	30	21-31	600-1100	140-230	11-17	--
Arundo Donax L.	43.2	20.5	17.2	1168	248	9.4	3.24



Fig. 1 Natural giant cane fiber mat after drying it for 12 hours at 70°C

laminated composite made from giant cane fiber is thought to be a potential candidate for the making laminates having structural usefulness. Fig. 1 shows the natural giant cane fiber mat after drying it for 12 hours at 70°C.

2.2 Matrix material

The matrix material utilized in the fabrication is epoxy resin Lapox-12 which has been obtained from Atul Chemical, India. It is moderately viscous (9000-12000 mPa.s at 25°C) and is used as the continuous stress transfer medium in the fabrication of composite laminate. A comparatively lower viscous hardener K-6 is added in 10:1 proportion by weight to the epoxy. The Lapox-12 epoxy and K-6 hardener have a good melt flow index, thermal stability, longer working time and high cure shrinkage stability than polyesters vinyl esters and poly propylene. The Lapox-12 epoxy is transparent and thereby imparts the natural looks of the fiber mats to the laminated composite fabricated using it.

2.3 Filler: Zirconia-toughened mullite (ZTM)

The Zirconia-toughened mullite (ZTM) ceramics has been prepared by reaction-sintering of mixtures of alumina and zirconia. The use of very fine particles and the choice of fast heating rates favor densification in comparison with mullitization. Re-associated zirconia must be preferred over dissociated one. The alumina to silica ratio is a critical parameter. The 75% Al₂O₃ composition shows the lowest room-temperature mechanical strength and the 68% composition the highest. ZrO₂ inclusions do not sensibly improve strength but they increase room-temperature toughness by more than 50%. At high-temperature, the mechanical properties are taken down by the low-viscosity of impure silica, iron oxide being particularly damaging.

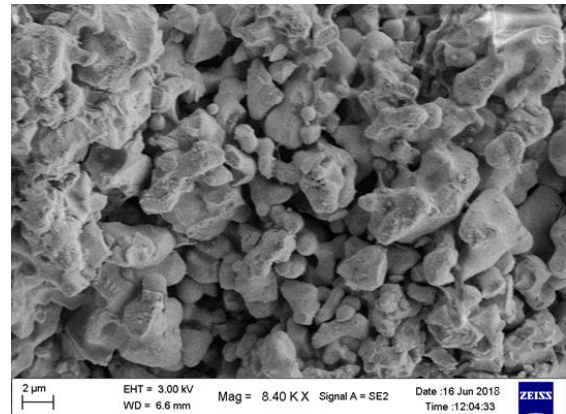


Fig. 2 SEM micrograph of ZTM filler

Table 2 Properties of epoxy, hardener, giant cane fiber mat and ZTM filler

Materials	Grade	Characteristics
Epoxy	Lapox L-12	Density = 1.1gm/cc Viscosity = 9,000-12,000 mPa.s
Hardener	K-6	Density=1gm/cc Refractive index=1.494 -1.50 (at 25°C)
Giant cane fiber mat	---	Weave type [+45°/-45°] Density = 0.95gm/cc Width = 3.7-4.0 mm Thickness = 0.3-0.4mm Specific gravity= 0.5-0.7
Zirconia-toughened mullite (ZTM)	---	Off white powder Non-soluble in water Excellent chemical and corrosion resistance Shape: irregular size Density=5.68g/cc Melting temp. = 2715°C Boiling point=4300°C Refractive index=2.13

The ZTM ceramics provide fairly good long-term thermal stability because the mullite has low thermal expansion coefficient ($\sim 5 \times 10^{-6} / ^\circ\text{C}^{-1}$), low thermal conductivity ($\sim 2\text{W/m}^\circ\text{C}$), chemical inertness, thermal stability and mainly because of its high creep resistance. The oxidation product of mullite always contains an (alumino-silicate + mullite) phase, which remains protective because of viscous flow relaxation of volume-change-induced stress. Mullite ceramics toughen on the addition of ZrO₂ particles. This toughening of mullite by ZrO₂ is understood to be a result of the transformation of t-ZrO₂ to m-ZrO₂ (transformation toughening) and micro crack formation around m-ZrO₂ (micro-crack toughening) during crack propagation. The

Table 3 Designations of composite specimens made from giant cane fiber epoxy with different wt. % of ZTM filler

Group	Designation	Fiber orientation	Wt. % of filler	
Untreated fiber mat	P0		0	
	P1		2.5	
	P	P2	[+45 ⁰ /-45 ⁰ /+45 ⁰]	5
		P3		7.5
		P4		10
		Q0		0
	Q	Q1		2.5
		Q2	[0 ⁰ /90 ⁰ /0 ⁰]	5
		Q3		7.5
		Q4		10
Treated fiber mat		R0		0
	R1		2.5	
	R	R2	[+45 ⁰ /-45 ⁰ /+45 ⁰]	5
		R3		7.5
		R4		10
		S0		0
	S	S1		2.5
		S2	[0 ⁰ /90 ⁰ /0 ⁰]	5
		S3		7.5
		S4		10

SEM micrograph (Fig. 2) of filler particle was carried out and some of its properties were studied from the analysis which is listed in Table 2.

2.4 Fabrication of composite laminate

The woven giant cane fiber mats are treated with 5% NaOH solution for 6 hours and maintained at 40°C. The giant cane fiber mats are then dried for 12 hours in drying oven at 70°C to remove moisture content before being used for the actual molding process. The epoxy resin (Lapox L-12) is applied on both the side of the fiber mats using a paint brush thoroughly. The ZTM filler in five different weight proportions (i.e., 0, 2.5, 5, 7.5 and 10) and the hardener (K-6) are added (10:1 by weight) to the matrix and mixed thoroughly before they are being applied to the fiber mats. The mixture is stirred till it becomes little warm. This happens because of the exothermic reaction taking place during resin curing. The composite laminate is fabricated by hand lay-up technique and was cured under a load of 50 kg for 24 hrs. Then, this cast was cured further in air for another 24 hours (after they are removed from the mold). Specimens of suitable dimensions were cut using a diamond cutter for characterization. Extreme care has been taken to maintain uniformity and homogeneity of the laminated composites. A number of laminated composite specimens made with giant cane fiber mats are prepared by varying the weight percentage of ZTM in them. The specimens are also prepared from both treated and untreated fiber mats in two different fiber orientation angles, i.e., [+45⁰/-45⁰/+45⁰] and

[0⁰/90⁰/0⁰]. The samples cut from the laminates are designated as mentioned in Table 3 for clear distinction. The designations P, Q represent the composite specimen made with the untreated fiber mats having [+45⁰/-45⁰/+45⁰] and [0⁰/90⁰/0⁰] fiber orientations, respectively. The designations R, S represent the composite specimens made with the NaOH treated fiber mats having [+45⁰/-45⁰/+45⁰] and [0⁰/90⁰/0⁰] fiber orientations, respectively.

3. Mechanical characterization

In order to study the different physical and mechanical properties of prepared laminated composite specimen, the following tests have been carried out as per the ASTM standards: (a) Scanning Electron Microscopy (SEM) using Jeol, Japan, JSM-6390LV available at BIT Mesra, (b) Vicker's microhardness test using Zwick Roell, ZHV 30, (c) Tensile test and (d) Interlaminar shear strength (ILSS) test using Universal Testing Machine, Zwick Roell at IIT Bhubaneswar, (e) Impact strength test at KIIT, Bhubaneswar.

3.1 Density and void fraction

The giant cane fiber reinforced composites consists of fiber, matrix and the ZTM particulate filler. Eq. (1) (Satapathy *et al.* 2010) is used to compute the theoretical density of the composites in terms of weight fractions of the individual components

$$\rho_{ct} = \frac{1}{(W_f/\rho_f) + (W_m/\rho_m) + (W_p/\rho_p)} \quad (1)$$

Where, ρ and W represents the density and weight fraction, respectively. The suffixes m, f, p and ct stand for the matrix, fiber, filler and the bio-composite material, respectively.

The actual density (ρ_{ce}) of the composite is found experimentally by using the water-immersion technique. The volume fraction of the voids (V_v) present in the composites is calculated as per Eq. (2) (Satapathy *et al.* 2010)

$$V_v = \frac{\rho_{ct} - \rho_{ce}}{\rho_{ct}} \quad (2)$$

3.2 Scanning electron microscopy (SEM)

The surfaces of the composite samples are scanned directly under the SEM. The samples are mounted on carbon stubs. To improve the conductivity of the samples, a skinny film of gold is vacuum-evaporated on them before the photomicrographs are taken.

3.3 Micro hardness

Vickers hardness tests are carried out for the composite specimens made with different weight percentage of filler in Zwick Roell (ZHV 30) microhardness tester as per ASTM E92 test procedure. Pyramid type diamond indenter is used

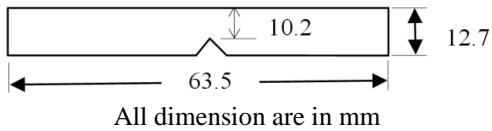


Fig. 3 Geometry of the impact test specimen

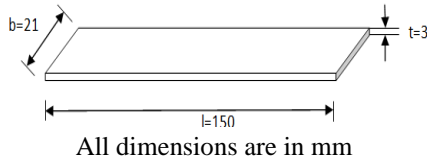


Fig. 4 Geometry of the tensile test specimen

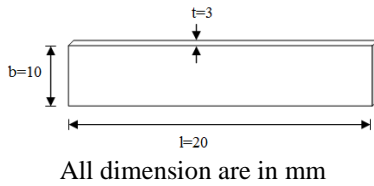


Fig. 5 Geometry of the ILSS test specimen

with load of 200 gram force (gf). The hardness values are measured at various locations randomly on the surface of the composite laminate.

3.4 Impact test

The impact tests are carried out to evaluate the toughness of the material. These tests also give an idea about the ballistic performance of the laminate. Pendulum impact tests (ASTM D256) are carried out on specimens having V-notch with depth of 2.5 mm and notch angle of 45° . The geometry of the specimen is illustrated in Fig. 3. The impact energy absorbed in each specimen is recorded from the digital readout screen.

3.5 Tensile test

Tensile strength is one of the significant attributes of composite laminates for evaluating their load carrying capability. Tensile tests of 100 different laminated composite specimens as per the designation given in Table 3 with varied percentages of the filler content made with both treated and untreated fibers for two extreme fiber angles i.e., $[+45^\circ/-45^\circ/+45^\circ]$ and $[0^\circ/90^\circ/0^\circ]$ have been conducted. The geometry and dimensions of tensile specimen are given in the Fig. 4. The specimens are cut from the laminates as per the ASTM (D3039) standard using a diamond cutter. The displacement based uniaxial tensile load at a loading rate of 2 mm/min is applied to the specimen in a Universal Testing Machine (Zwick Roell).

3.6 Interlaminar shear strength (ILSS)

In reality, the structural members made out of composite laminates are subjected to complex loading conditions. Many times the applied loading direction is off-axis and not

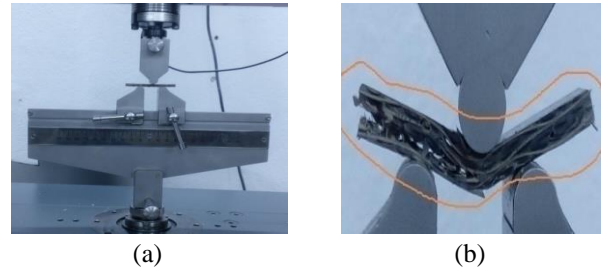


Fig. 6 ILSS test of the composite specimen: (a) specimen at beginning, (b) specimen after delamination

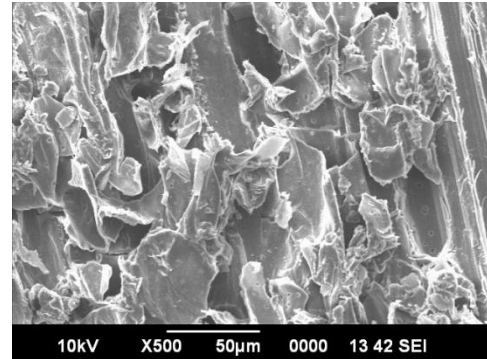


Fig. 7 SEM micrograph of untreated composite sample with filler

parallel to the fibers present in the composites. The structural integrity in shear and bending loading depends on the interlaminar shear strength of the member. Hence, investigation of ILSS of all types of the fabricated giant cane fiber epoxy based bio-composites such as P_x , Q_x , R_x and S_x ($x=0, 1, 2, 3, 4$ as in Table 3) are carried out as per DIN EN 2377 standard. The specimens for ILSS test, geometry and dimensions as shown in Fig. 5, are cut from the laminates using a diamond cutter. The displacement of the applied load speed is 5 mm/min.

The ILSS tests are performed on the Universal Testing Machine (Zwick Roell) using the fixtures as shown in the Fig. 6. It is seen that the delamination of the composite has taken place during the ILSS test.

4. Results and discussion

The morphology of the composite reinforced with untreated and treated fiber surfaces has been studied using an SEM. The surfaces of untreated fiber appear to be rough as shown in Fig. 7. This may be due to the presence of lignin, wax, oil and other impurities which are removed with alkali treatment.

The surfaces of the treated fiber are shown in Fig. 8. These clean surfaces are expected to provide a direct bonding between the fiber and the matrix.

4.1 Density and void fraction

The theoretical densities (computed using Eq. (1)), measured densities, and the corresponding void fractions (computed using Eq. (2)) of the giant cane fiber reinforced

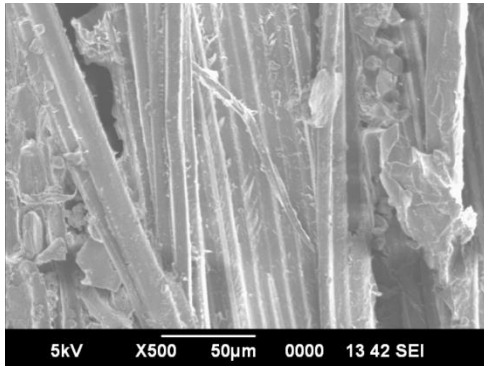


Fig. 8 SEM micrograph of treated composite sample with filler

Table 4 Densities and void fractions of the composites specimens

Composites	Theoretical density (ρ_{ct}) (g/cc)	Measured density (ρ_{ce}) (g/cc)	Volume fraction of voids V_v (%)
P0	1.170	1.150	1.709
P1	1.180	1.160	1.694
P2	1.190	1.170	1.680
P3	1.202	1.180	1.830
P4	1.213	1.200	1.071
R0	1.200	1.190	0.833
R1	1.180	1.170	0.847
R2	1.170	1.160	0.854
R3	1.150	1.130	1.730
R4	1.140	1.130	0.877

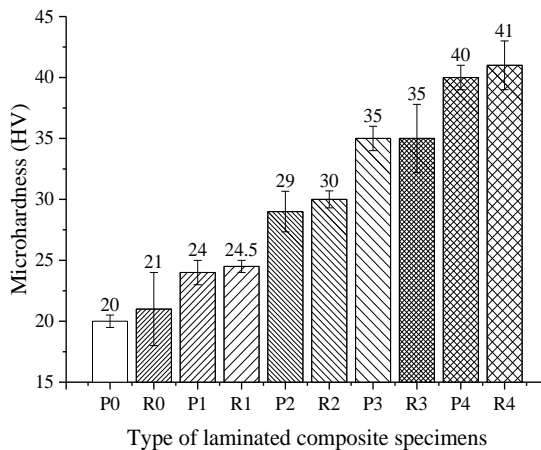


Fig. 9 Microhardness values of the laminated composite specimens

laminated composites are presented in Table 4. It may be noted that the theoretically and the experimentally determined density values of the giant cane fiber composite are not equal to each other due to the voids and pores present in the composites. It can be observed from Table 4 that the variation of density of composite specimens made with untreated and treated fiber mats are small. The density also does not vary with change of fiber orientation angle.

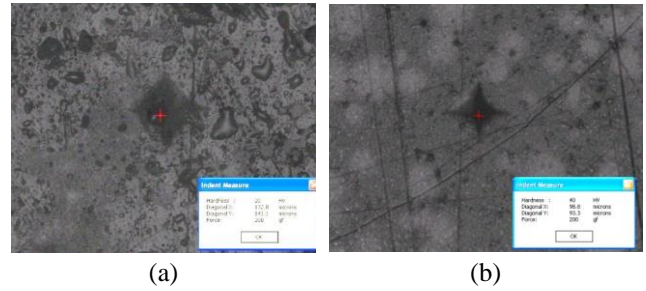


Fig. 10 Hardness value for: (a) no filler (P0) and (b) filler (P4) samples

So, it can be considered that density of P_x is same as Q_x and density of R_x is same as that of S_x .

4.2 Microhardness

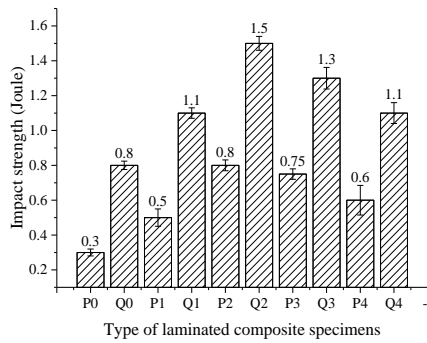
The microhardness of the prepared samples is evaluated. Fig. 9 shows the average of micro hardness values of various specimens made from both untreated and treated fibers having different weight percentages of filler contents. Five samples for each category i.e., a total of 100 (20×5) of samples are tested.

There is a small increase in the hardness values in composite specimens only because of the treatment of the fibers with NaOH. The average hardness values of specimens P0 and R0 are 20 and 21 HV respectively. In contrast, the average bulk hardness of the specimen increases almost linearly with the increment of filler percentage in the specimens. This increasing trend in hardness values may be attributed to the inclusion of uniformly distributed harder particles in the continuous resin matrix. This may also be governed as per the rules of mixture theory. The maximum value of the average hardness obtained is 41HV in specimen (R4) having 10 wt.% of the ZTM. However, the change in fiber orientation angle of the fibers mat in the composite does not influences the hardness value. The image captured for microhardness value of the composite samples P0 and P4 are shown in Fig. 10 (a) and (b), respectively.

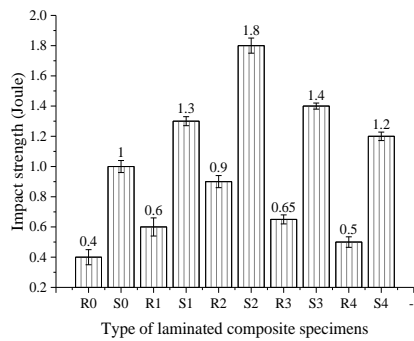
4.3 Impact strength

Fig. 11(a) and (b) shows the impact strength values of the composite specimens made from both untreated and treated fiber mats. At least five tests for each category (as per the category described in Table 3) of the specimens are carried out. It can be observed from Fig. 11 that the impact strength is more for composite specimens with $[0^0/90^0/0^0]$ fiber orientation configurations than that of $[+45^0/-45^0/+45^0]$ configurations.

This may be due to the reason that more number of fibers is aligned transversely to the impact force in them. Again, impact strength increases by the addition of filler content up to a certain limit (i.e., up to 5 wt. % of filler), and decreases thereafter. This may be due to the presence of higher volume fractions of the voids and problem related to non-uniform dispersion of filler in the giant cane fiber based composites. The composite specimens made with



(a)



(b)

Fig. 11 Impact strength of different untreated and treated composite specimens: (a) $[+45^0/-45^0/+45^0]$, (b) $[0^0/90^0/0^0]$

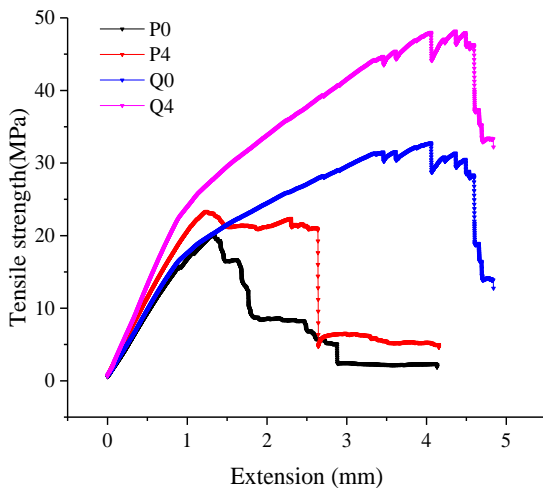


Fig. 12 Tensile strength of laminated composites specimens (P0, P4, Q0 & Q4)

treated giant cane fiber mats have better impact strength than the corresponding specimens made with untreated fibers. More weighting area acts as better stress transfer media and hence possess better energy absorption capacity due to impact.

4.4 Tensile strength

The typical results of the tensile tests (stress-strain behavior) carried out as per ASTM (D3039) standard for

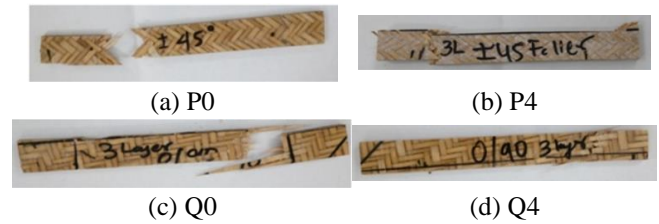


Fig. 13 The broken sample after the tensile test showing pull out of untreated fiber mats: (a) P0, (b) P4, (c) Q0 and (d) Q4

specimens P0, P4, Q0 and Q4 are shown in Fig. 12. The locations having comparatively higher ZTM filler contents (particularly more than 10 wt. %) are the sources of stress concentrations. The presence of higher number of such stress concentration location reduces the energy absorbing capacity of the composite during test. The failure of the tensile specimens happens in a very complex manner. The failure happens due to the combined effect of phenomena such as fiber breaking, matrix cracking, delamination and fiber pull out during the tensile test.

The average values of tensile strengths of all the test samples are shown in Fig. 14 and the broken samples after the tests are shown in Fig. 13.

4.4.1 For untreated $[+45^0/-45^0/+45^0]$ fiber orientation

The maximum tensile strength the specimen P0 can withstand before failure is around 22 MPa as observed from Fig. 12. The failure of the specimen does not take place immediately after the maximum tensile strength is attained but happens with substantial extension. The extension region from 1.2 to 2.8 mm (Fig. 12) shows multiple load drops.

These load drops in the strength-extension graph may be happening due to sequential breaking of fibers in different layers. The extensions from 3 mm to 5 mm may be due to pulling out of the fibers from mesh of the woven mat. It is observed from the tensile test for the specimen P0 that the fiber pullout from the mesh $[+45^0/-45^0/+45^0]$ is the major resistance offered to the deformation causing extensions from 3 mm to 5 mm upon loading. Whereas, in case of the tensile test of the specimens (P4), the strengths are higher and there is a prominent yield region without much of load drop followed by sudden load drop due to fiber pull outs. But, the higher strength of the specimen (P4) may be due to the resistance to deformation by the mechanical anchorage and the ploughing resistance of the embedded harder filler particles in these types of specimens. The filler particles attached to the fiber mats provide more mechanical anchorages to the sliding phenomenon of one layer over the other during loading in the laminated composite specimens. Here, breakages of the fibers are also seen along with the pulled out fibers shown in Fig. 13(a) and (b). While the extension is from 1 mm to 2.5 mm, the decrease in slope of tensile strength can be observed. It is due to the adhesion failure and delamination related failure happening in the interlaminar region followed by no extension due to breakage across the cross section.

The average strength of samples with fillers has higher

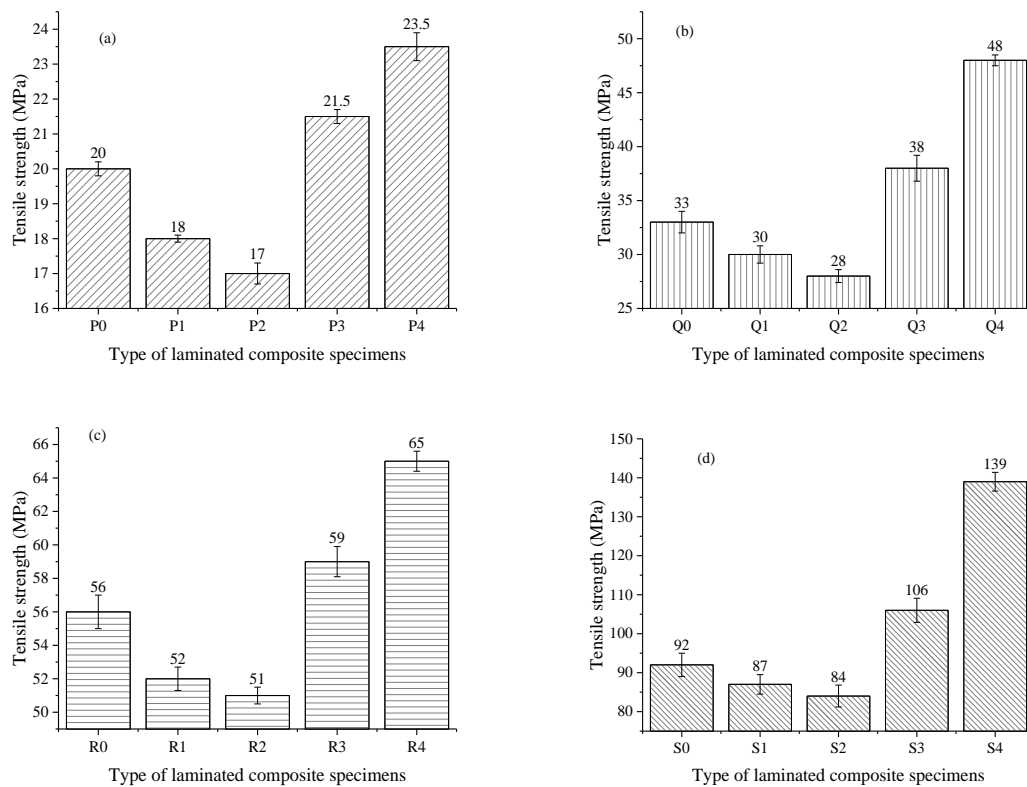


Fig. 14 Tensile strength of different laminated composite specimens: (a) P_x, (b) Q_x, (c) R_x and d) S_x

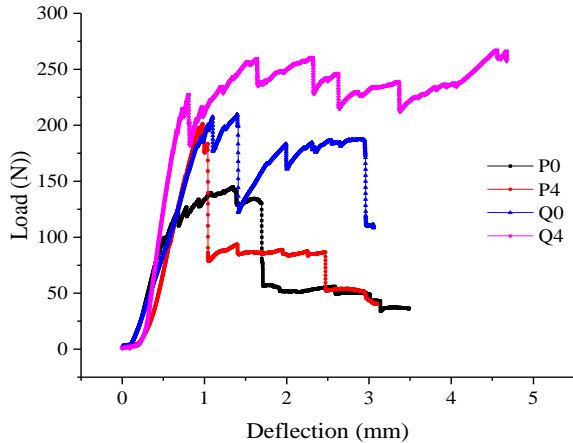


Fig. 15 Load-deformation behavior of specimens (P0, P4, Q0, and Q4) made from untreated fiber mats during the interlaminar shear strength test as per DIN EN 2377

values than that of specimens made with no filler. Further, the strength of specimens with higher weight percentage of ZTM (i.e., beyond 10 wt. %) decreases because of the occurrence of large voids (non-wetting of fibers mats) appearing in the casting of laminates.

4.4.2 For untreated $[0^0/90^0/0^0]$ fiber orientation

Higher strengths are observed for the specimens made in $[0^0/90^0/0^0]$ compared to the specimens made in $[+45^0/-45^0/+45^0]$ configuration. This may be reasoned out as the principal directions of more fibers in the mats are aligned

along the loading directions as fibers are the principal load carrying members. Here, the failure is mainly due to the breaking of the longitudinally aligned fibers and followed by the minor contributions from fiber pull out shown in Fig. 13(c) and (d). The specimen Q4 has higher strength due to the better anchorage resistance to pull out in addition to the breaking of longitudinal fibers. There is a sudden load drop as the specimens Q0 and Q4 fail across the cross-section and the same can be observed from Fig. 12. No distinct yield region is observed and fracture takes place almost suddenly beyond the critical point. Multiple load drops for the specimens Q0 and Q4 are due to the sequential breaking of the fibers after critical point. The summary of tensile test results of all the specimens shown in Fig. 14 is as follows:

(i) The average tensile strength for specimens with no filler P0, Q0, R0 and S0 are 20, 33, 56 and 92 MPa, respectively. The addition of 0 to 5 wt. % of filler decreases the tensile strength. The filler particles are the stress concentration locations in the specimen P1 and P2 than specimen P0. Thereby, lower strength is observed with increasing percentage of filler from P0 to P2.

(ii) For higher weight percentage of the filler in specimens (i.e., for 7.5 and 10 wt. % of the filler) the tensile strength increases. This increase in strength in these specimens with 7.5 to 10 wt. % of the filler may be due to the inclusion of higher number of filler particulates in specimens P3, P4, Q3, Q4, R3, R4, and S3, S4 respectively. However, further addition of fillers in specimens P3 and P4 creates comparatively larger number of stress concentration locations than specimens P1 and P2.

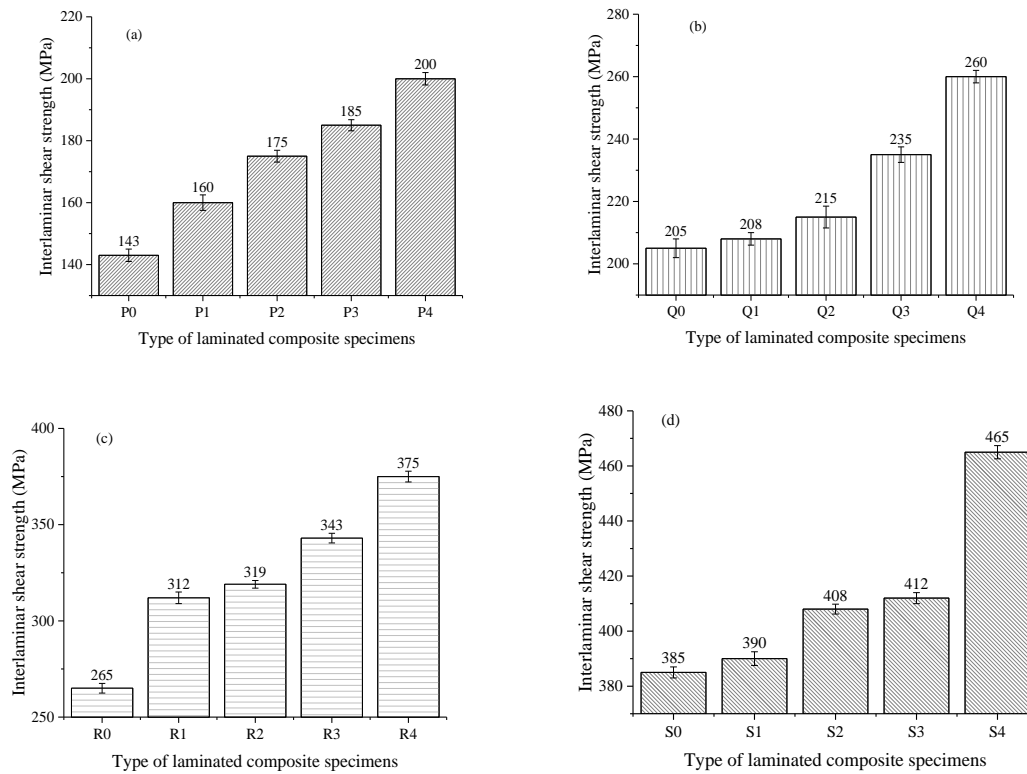


Fig. 16 ILSS test of different laminated composite specimens: (a) P_x , (b) Q_x , (c) R_x and d) S_x

While the specimen undergoing straining due to loading the crack nucleating from these stress locations may interfere with each other during propagation under loading due to their higher density in these specimens. Hence, more strain energy is required to be spent in growth of multiple interfering crack fronts. Apart from the above reasons, further addition of fillers (beyond 5%) having higher stiffness values than the matrix materials may contribute to increase in strength according to the rules of mixture. Exponential increasing trend in the tensile strength test is observed. There are deviations in the strength during tensile test in each category. These variations may be due to the presence of void contents and non-uniform wetting of fiber mats and anisotropy introduced during the manufacturing process. From the above listed observations in the light of results presented in Fig. 14, the influence of filler addition on specimens is fairly recognizable to be non-linear. The treatments of fiber mats with NaOH influences the strength and are due to better adhesion characteristics of the fiber mats with the matrix. Hence, higher strength is observed from the test results in specimens R_x and S_x .

4.5 Interlaminar shear strength

The typical load-deflection curves of the ILSS tests are shown in Fig. 15. The tests are carried out for the specimens P0, P4, Q0, and Q4 in a UTM (Zwick Roell) as per the ASTM standard (DIN EN 2377). The maximum loads in ILSS for specimen type P0 and Q0 are 143N and 208.8N, and for specimen type P4 and Q4 are 203.6N and 270N,

respectively. The average values of the ILSS evaluated from the tests for specimens belonging to all the categories (as described in Table 3) are shown in Fig. 16. The following observations are made from the tests of 100 samples:

(i) With the addition of the ZTM in the range 0 to 5 wt. percentage, there is an increase in ILSS of the laminated composite. The increments in the average ILSS values in the all other specimens are summarized in the Fig. 16.

(ii) Further, increase in weight percentage of the filler (i.e., for the specimens made with 7.5 to 10 wt. % the filler) of the average interlaminar shear strengths increase and the same can be observed from Fig. 16.

From the above listed observations, it is concluded that the influence of filler addition on specimens is fairly recognizable to be linearly increasing with the increase of the filler content. This may be reasoned out as that the discontinuous particulates (ZTM) sites are evenly spread in the inter-laminar regions obstructing the sliding of one layer over the other during loading. So, the presence of more numbers of the filler particulates creates more number of obstructing sites in the inter-laminar regions of the specimens. Hence, these obstructing sites may be contributing to the increase in ILSS of specimens with higher weight percentage of the filler. Hence, higher strength is observed from the test results in specimens R_x and S_x . The ILSS of the $[0^0/90^0/0^0]$ specimens are higher than $[+45^0/-45^0/+45^0]$ specimens because of the alignment of 90^0 fiber in the lamina to the loading axis possess more anchorage than the 45^0 oriented fibers when one layer is

sliding with respect to the adjacent layer during the ILSS test. It has been observed that inter laminar shear strength of treated fiber composites is approximate two times greater than the untreated fiber composites due to better adhesion of the fiber mats to the matrix.

5. Conclusions

The giant cane (*Arundinaria*) fiber epoxy composites filled with zirconia-toughened mullite (ZTM) were successfully fabricated using hand lay-up technique. The physical and mechanical properties i.e., density, microhardness, impact strength, tensile strength and interlaminar shear strength, of the composite laminates were evaluated experimentally by following the appropriate ASTM standards. The experimental observation reveals that a limited inclusion of the ZTM as filler in the giant cane fiber based composite improves the microhardness, impact strength, tensile strength, and interlaminar shear strength (ILSS). Thus, the composite laminates can be customized depending on the structural requirement by varying weight fractions of treated giant cane fiber mat, ZTM, angle of fiber orientation and number of layers. The study clearly indicates that the tensile strength and ILSS values are higher for 10 wt. % of filler added with the treated fiber. Again, the tensile strength is higher for the balanced laminate $[0^0/90^0/0^0]$ i.e., 51.08% in comparison to the angle-ply $[+45^0/-45^0/+45^0]$. Moreover, the ILSS value are found to be 41.5 % more for the angle-ply laminates in comparison to balanced laminates. However, the impact strength of the angle-ply laminates of untreated fibers is higher and its value is 166.67 % for 10 wt. % of filler. But, the microhardness value gradually increases with an increasing filler percentages and has a maximum of 41HV for 10 wt. % of filler of untreated fibers. Further, the use of ZTM as filler reduces the load on the environment which otherwise may has been disposed to the environment causing pollution. It can be inferred that the ZTM filled composite laminate can be adopted for the low strength type structural material.

References

- Amnieh, H.B., Zamzam, M.S. and Kolahchi, R. (2018), "Dynamic analysis of non-homogeneous concrete blocks mixed by SiO₂ nanoparticles subjected to blast load experimentally and theoretically", *Constr. Build. Mater.*, **174**, 633-644.
- Arani, A.J. and Kolahchi R. (2016), "Buckling analysis of embedded concrete columns armed with carbon nanotubes", *Comput. Concrete*, **17**(5), 567-578.
- Bilouei, B.S., Kolahchi, R. and Rabani, B.M. (2016), "Buckling of concrete columns retrofitted with nano-fiber reinforced polymer (NFRP)", *Comput. Concrete*, **18**(5), 1053-1063.
- Bisen, H.B., Hirwani, C.K., Satankar, R.K., Panda, S.K. and Patel, B. (2018), "Numerical study of Frequency and deflection responses of natural fiber (Luffa) reinforced polymer composite and experimental validation", *J. Nat. Fib.*, 1-15.
- Biswas, S., Deo, B., Patnaik, A. and Satapathy, A. (2011), "Effect of fiber loading and orientation on mechanical and erosion wear behaviors of glass-epoxy composites", *Polym. Compos.*, **32**(4), 665-674.
- Cruz, R.B., Juniora, E.P., Monteiroa, S.N. and Louroa, L.H. (2015), "Giant bamboo fiber reinforced epoxy composite in multilayered ballistic armor", *Mat. Res.*, **18**(2), 70-75.
- Cunha, J., Foltete, E. and Bouhaddi, N. (2008), "Characterization of elastic properties of pultruded profiles using model updating procedure with vibration test data", *Struct. Eng. Mech.*, **30**(4), 481-500.
- Fiore, V., Botta, L., Scaffaro, R., Valenza, A. and Pirrotta, A. (2014b), "PLA based biocomposites reinforced with *Arundo donax* fillers", *Compos. Sci. Technol.*, **105**, 110-117.
- Fiore, V., Scalici, T. and Valenza, A. (2014), "Characterization of a new natural fiber from *Arundo donax* L. as potential reinforcement of polymer composites", *Carbohydr. Polym.*, **106**, 77-83.
- Fiore, V., Scalici, T., Vitale, G. and Valenza, A. (2014a), "Static and dynamic mechanical properties of *Arundo Donax* fillers-epoxy composites", *Mater. Des.*, **57**, 456-464.
- Gabarron, A.M., Flores, Y.J.A., Pastor, J.J., Berna Serna, J.M., Arnold, L.C. and Medrano, F.J. (2014), "Increase of the flexural strength of construction elements made with plaster (calcium sulfate dihydrate) and common reed (*Arundo donax* L.)", *Constr. Build. Mater.*, **66**, 436-441.
- Gonçalves, A.M., Ferreira, J.G., Guerreiro, L. and Branco, F.A. (2015), "Experimental characterization of timber framed masonry walls cyclic behaviour", *Struct. Eng. Mech.*, **53**(2), 189-204.
- Gurunathan, T., Mohanty, S. and Nayak, S.K. (2015), "A review of the recent developments in biocomposites based on natural fibres and their application perspectives", *Compos. Part A*, **77**, 1-25.
- Hajmohammad, M.H., Farrokhanian, A. and Kolahchi, R. (2018b), "Smart control and vibration of viscoelastic actuator-multiphase nanocomposite conical shells-sensor considering hygrothermal load based on layer wise theory", *Aerosp. Sci. Technol.*, **78**, 260-270.
- Hajmohammad, M.H., Kolahchi, R., Zarei, M.S. and Maleki, M. (2018a), "Earthquake induced dynamic deflection of submerged viscoelastic cylindrical shell reinforced by agglomerated CNTs considering thermal and moisture effects", *Compos. Struct.*, **187**, 498-508.
- Hajmohammad, M.H., Maleki, M. and Kolahchi, R. (2018e), "Seismic response of underwater concrete pipes conveying fluid covered with nano-fiber reinforced polymer layer", *Soil Dyn. Earthq. Eng.*, **110**, 18-27.
- Hajmohammad, M.H., Zarei, M.S., Nouri, A. and Kolahchi, R. (2017a), "Dynamic buckling of sensor/functionally graded-carbon nanotube reinforced laminated plates/actuator based on sinusoidal-viscopiezoelasticity theories", *J. Sandw. Struct. Mater.*, 1099636217720373.
- Jena, H., Pandit, M.K. and Pradhan, A.K. (2013), "Effect of cenosphere on mechanical properties of bamboo-epoxy composites", *J. Reinf. Plast. Compos.*, **32**(11), 794-801.
- John, M.J., Francis, B., Varughese, K.T. and Thomas, S. (2008), "Effect of chemical modification on properties of hybrid fiber biocomposites", *Compos. Part A*, **39**(2), 352-363.
- Karahancer, S., Eriskin, E., Sarioglu, O., Capali, B., Saltan, M. and Terzi, S. (2016), "Utilization of *Arundo Donax* in hot mix asphalt as a fiber", *Constr. Build. Mater.*, **125**, 981-986.
- Kim, S., Jung, H., Kim, Y. and Park, C. (2018), "Effect of steel fiber volume fraction and aspect ratio type on the mechanical properties of SIFCON-based HPFRCC", *Struct. Eng. Mech.*, **65**(2), 163-171.
- Kolahchi, R. (2017d), "A comparative study on the bending, vibration and buckling of viscoelastic sandwich nano-plates based on different nonlocal theories using DC, HDQ and DQ methods", *Aerosp. Sci. Technol.*, **66**, 235-248.
- Kolahchi, R. and Bidgili, A.M. (2016a), "Size-dependent

- sinusoidal beam model for dynamic instability of single-walled carbon nanotubes”, *Appl. Math. Mech. Engl. Ed.*, **37**(2), 265-274.
- Kolahchi, R., Hosseini, H. and Esmailpour, M. (2016), “Differential cubature and quadrature-Bolotin methods for dynamic stability of embedded piezoelectric nanoplates based on visco-nonlocal-piezoelectricity theories”, *Compos. Struct.*, **157**, 174-186.
- Kolahchi, R., Keshtegar, B. and Fakhar, M.H. (2017a), “Optimization of dynamic buckling for sandwich nanocomposite plates with sensor and actuator layer based on sinusoidal-visco-piezoelectricity theories using Grey Wolf algorithm”, *J. Sandw. Struct. Mater.*, 1099636217731071.
- Kolahchi, R., Safari, M. and Esmailpour, M. (2016 b), “Dynamic stability analysis of temperature-dependent functionally graded CNT-reinforced visco-plates resting on orthotropic elastomeric medium”, *Compos. Struct.*, **150**, 255-265.
- Kolahchi, R., Zarei, M.S., Hajmohammad, M.H. and Nouri, A. (2017c), “Wave propagation of embedded viscoelastic FG-CNT-reinforced sandwich plates integrated with sensor and actuator based on refined zigzag theory”, *Int. J. Mech. Sci.*, **130**, 534-545.
- Kolahchi, R., Zarei, M.S., Hajmohammad, M.H. and Oskouei, A.N. (2017b), “Visco-nonlocal-refined Zigzag theories for dynamic buckling of laminated nanoplates using differential cubature-Bolotin methods”, *Thin-Wall. Struct.*, **113**, 162-169.
- Kushwaha, P. and Kumar, R. (2008), “Enhanced mechanical strength of BFRP composite using modified bamboos”, *J. Reinf. Plast. Compos.*, **28**(23), 51-59.
- Manalo, A.C., Wani, E., Zukarnain, N.A., Karunasena, W. and Lau, K.T. (2015), “Effects of alkali treatment and elevated temperature on the mechanical properties of bamboo fibre-polyester composites”, *Compos. Part B*, **80**, 73-83.
- Mir, S.S., Nafsin, N., Hasan, M., Hasan, N. and Hassan, A. (2013), “Improvement of physico-mechanical properties of coir-polypropylene biocomposites by fiber chemical treatment”, *Mater. Des.*, **52**, 251-257.
- Perrier, A., Touchard, F., Chocinski-Arnault, L. and Mellier, D. (2017), “Quantitative analysis by micro-CT of damage during tensile test in a woven hemp/epoxy composite after water ageing”, *Compos. Part A, Appl. Sci. Manuf.*, **102**, 18-27.
- Sanjay, M.R., Arpitha, G.R., Naik, L.L., Gopalakrishna, K. and Yogesha, B. (2016), “Applications of natural fibers and its composites: An overview”, *Nat. Res.*, **7**(3), 108-114.
- Satapathy, A.K., Jha, A.K., Mantry, S., Singh, S.K. and Patnaik, A. (2010), “Processing and characterization of jute-epoxy composites reinforced with SiC derived from rice husk”, *J. Reinf. Plast. Compos.*, **29**(18), 2869-2878.
- Sawpan, M.A., Pickering, K.L. and Fernyhough, A. (2011), “Improvement of mechanical performance of industrial hemp fibre reinforced polylactide biocomposites”, *Compos. Part A, Appl. Sci. Manuf.*, **42**(3), 310-319.
- Scalici, T., Fiore, V. and Valenza, A. (2016), “Effect of plasma treatment on the properties of Arundo Donax L. leaf fibres and its bio-based epoxy composites: A preliminary study”, *Compos. Part B*, **94**, 167-175.
- Sepe, R., Bollino, F., Boccarusso, L. and Caputo, F. (2018), “Influence of chemical treatments on mechanical properties of hemp fiber reinforced composites”, *Compos. Part B*, **133**, 210-217.
- Shokravi, M. (2017), “Buckling of sandwich plates with FG-CNT-reinforced layers resting on orthotropic elastic medium using Reddy plate theory”, *Steel Compos. Struct.*, **23**(6), 623-631.
- Shokravi, M. (2017), “Dynamic pull-in and pull-out analysis of viscoelastic nanoplates under electrostatic and Casimir forces via sinusoidal shear deformation theory”, *Microelectr. Rel.*, **71**, 17-28.
- Yan, L., Chouw, N., Huang, L. and Kasal, B. (2016), “Effect of alkali treatment on microstructure and mechanical properties of coir fibres, coir fibre reinforced-polymer composites and reinforced-cementitious composites”, *Constr. Build. Mater.*, **112**, 168-182.
- Zamanian, M., Kolahchi, R. and Bidgoli, M.R. (2017), “Agglomeration effects on the buckling behaviour of embedded concrete columns reinforced with SiO₂ nano-particles”, *Wind Struct.*, **24**(1), 43-57.
- Zarei, M.S., Kolahchi, R., Hajmohammad, M.H. and Maleki, M. (2017), “Seismic response of underwater fluid-conveying concrete pipes reinforced with SiO₂ nanoparticles and fiber reinforced polymer (FRP) layer”, *Soil Dyn. Earthq. Eng.*, **103**, 76-85.

CC